Essential roles of zebrafish *bmp2a*, *fgf10*, and *fgf24* in the specification of the ventral pancreas

François Naye[a], Marianne L. Voz[a], Nathalie Detry[a], Matthias Hammerschmidt[b], Bernard Peers[a], and Isabelle Manfroid[a]

[a]Unit of Molecular Biology and Genetic Engineering, GIGA-Research, University of Liège, B-4000 Sart-Tilman, Belgium; [b]Institute of Developmental Biology, Cologne Excellence Cluster on Cellular Stress Responses in Aging-Associated Diseases, Center for Molecular Medicine Cologne, University of Cologne, D-50923 Cologne, Germany

ABSTRACT **In vertebrates, pancreas and liver arise from bipotential progenitors located in the embryonic gut endoderm. Bone morphogenic protein (BMP) and fibroblast growth factor (FGF) signaling pathways have been shown to induce hepatic specification while repressing pancreatic fate. Here we show that BMP and FGF factors also play crucial function, at slightly later stages, in the specification of the ventral pancreas. By analyzing the pancreatic markers *pdx1*, *ptf1a*, and *hlxb9la* in different zebrafish models of BMP loss of function, we demonstrate that the BMP pathway is required between 20 and 24 h postfertilization to specify the ventral pancreatic bud. Knockdown experiments show that *bmp2a*, expressed in the lateral plate mesoderm at these stages, is essential for ventral pancreas specification. *Bmp2a* action is not restricted to the pancreatic domain and is also required for the proper expression of hepatic markers. By contrast, through the analysis of *fgf10*$^{-/-}$; *fgf24*$^{-/-}$ embryos, we reveal the specific role of these two FGF ligands in the induction of the ventral pancreas and in the repression of the hepatic fate. These mutants display ventral pancreas agenesis and ectopic masses of hepatocytes. Overall, these data highlight the dynamic role of BMP and FGF in the patterning of the hepatopancreatic region.**

Monitoring Editor
Marianne Bronner-Fraser
California Institute of Technology

Received: Aug 2, 2011
Revised: Nov 23, 2011
Accepted: Dec 28, 2011

INTRODUCTION

Pancreas is an endodermal organ composed of endocrine and exocrine tissues that respectively produce hormones and digestive enzymes. During embryogenesis, pancreas arises from two buds developing from the dorsal and ventral aspects of the gut epithelium. The ventral pancreatic bud appears adjacent to the liver bud, and previous studies on mouse embryonic explants and in zebrafish revealed the presence of bipotential endodermal progenitors that can give rise to both organs (Deutsch *et al.*, 2001; Rossi *et al.*, 2001; Chung *et al.*, 2008). This cell fate decision is controlled by extrinsic factors released by the neighboring lateral plate mesoderm (LPM). Identification of such inducing stimuli is critical to the design of novel cellular therapies for pathologies affecting these organs.

In zebrafish, specification of the pancreatic region can be detected as early as 14 h postfertilization (hpf) through the activation of *pdx1* expression in midtrunk endoderm (Biemar *et al.*, 2001). The first *pdx1*-expressing cells, which are located near the medial line of the embryo just under the notochord, will delaminate to form the dorsal pancreatic bud by 24 hpf and will generate the first pancreatic endocrine cells. The first signs of hepatic development occur at 22 hpf with the activation of *prox1* and *hhex* expression in a segment of the gut endoderm anterior to the dorsal pancreatic bud (Ober *et al.*, 2006). These *prox1*$^{+}$/*hhex*$^{+}$ cells produce an outgrowth on the left side of the intestinal rod. The formation of this hepatic bud is quickly followed by the specification of the ventral pancreatic bud, which appears adjacent and posterior to the liver (Field *et al.*, 2003a). Indeed, *ptf1a* and *hlxb9la* (also named *mnr2a*)—the two earliest markers of the ventral pancreas—are detected at 32 hpf between the liver and dorsal pancreatic buds (Wendik *et al.*, 2004; Zecchin *et al.*, 2004). The *pdx1* homeobox gene, expressed in endocrine cells of the dorsal bud, is also detected in the adjacent

This article was published online ahead of print in MBoC in Press (http://www.molbiolcell.org/cgi/doi/10.1091/mbc.E11-08-0664) on January 4, 2012.

Address correspondence to: Bernard Peers (Bpeers@ulg.ac.be) and Isabelle Manfroid (Isabelle.manfroid@ulg.ac.be).

Abbreviations used: BMP, bone morphogenic protein; EHD, extrahepatic duct; EPD, extrapancreatic duct; FGF, fibroblasts growth factor; VPB, ventral pancreatic bud.

segment of intestinal rod, which encompasses the prospective ventral pancreatic bud. In zebrafish, the ventral pancreatic bud (VPB) generates the whole exocrine tissue comprising the acinar and ductal cells. The ventral and dorsal pancreatic buds eventually merge by 52 hpf to form the pancreas (Field *et al.*, 2003a, 2003b).

The ventral pancreatic and hepatic buds are induced by the adjacent mesodermal tissues through the release of signaling molecules such as fibroblast growth factors (FGFs) and bone morphogenic proteins (BMPs). However, conflicting data have been reported on the effect of these factors, revealing either an inducing or a repressing activity. For example, experiments on mouse embryonic explants showed that FGF from the cardiac mesoderm and BMP from the septum transversum are essential for the induction of liver markers and block pancreatic specification (Deutsch *et al.*, 2001; Rossi *et al.*, 2001). Similarly, FGFs and BMPs have also been shown in zebrafish to be essential for hepatic induction (Shin *et al.*, 2007), and *bmp2b* can specify liver at the expense of pancreas (Chung *et al.*, 2008). On the other hand, experiments with chicken embryonic explants indicate that BMP from the LPM is required for development of the ventral pancreas (Kumar *et al.*, 2003), and we reported that FGF signaling is essential to specify the ventral pancreatic bud in zebrafish embryos (Manfroid *et al.*, 2007). These contradictory results could be explained by a highly dynamic change in the inductive network. Indeed, Wandzioch and Zaret (2009) recently demonstrated that, whereas BMPs repress pancreatic specification at 3-4S in mouse embryos, they promote pancreatic fate a few hours later at 5-6S Another explanation could be that distinct members of the FGF and/or BMP ligand families have different activities. Thus a better understanding of liver and ventral pancreas development will require the identification of the BMP and FGF ligands expressed near the prospective hepatopancreatic region and their mutual relation.

In the present study, we show the crucial role of BMP pathway after 20 hpf for the specification of the ventral pancreatic bud in zebrafish embryos. We identify *bmp2a* as a crucial player in this induction and demonstrate its requirement for the activation of the first markers of the ventral pancreas (*ptf1a* and *hlxb9la*) as well as of the liver (*prox1* and *hhex*). In contrast, by analyzing these pancreatic and hepatic markers in double *fgf10*$^{-/-}$; *fgf24*$^{-/-}$ mutants, we find that both FGF10 and FGF24 ligands have completely opposed effect on the two organs, inducing all pancreatic markers while repressing hepatic markers. Thus our study provides new insights into the molecular mechanisms that initiate development of the liver and pancreas.

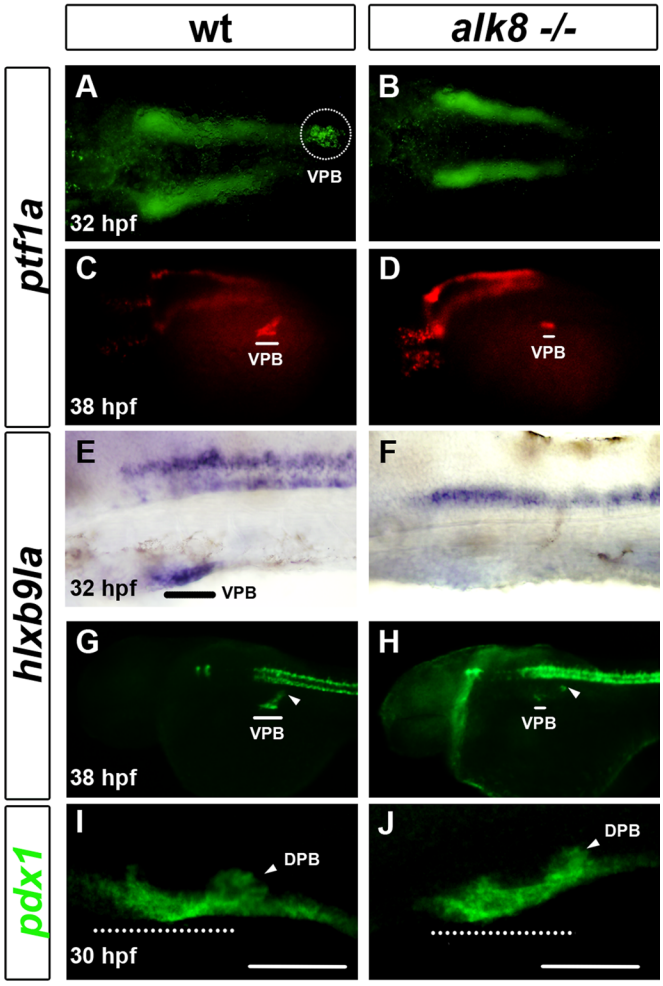

FIGURE 1: Decrease in BMP signaling leads to a delay in VPB specification and to a reduction in *ptf1a*$^{+}$ and *hlxb9la*$^{+}$ VPB progenitors. (A, B) Ventral view of *ptf1a* expression in wild-type (wt) sibling compared with *alk8* mutant (*alk8*$^{-/-}$) at 32 hpf. (C, and D) Lateral view of *ptf1a* expression in wt and *alk8* mutant at 36–38 hpf. (E–J) Lateral view of *hlxb9la* expression in wt and *alk8* mutant at 32 hpf (E, and H) and 36–38 hpf. (I, J). Lateral view of *pdx1* expression in wt and *alk8* mutant. White and black lines and white-dotted circle indicate the ventral pancreatic bud (VPB); white-dotted lines indicate the prospective ventral pancreatic bud; and white arrowheads indicate the dorsal pancreatic bud (DPB).

RESULTS

Requirement of BMP signaling in the specification of the ventral pancreatic bud

Involvement of BMP signaling in liver bud specification was previously investigated with *laf/alk8* mutants (Chung *et al.*, 2008). In addition, Chung *et al.* (2010) showed that VPB outgrowth was severely affected in *alk8* mutants, and *alk8* morphants have a hypoplasic ventral pancreas at 3 d postfertilization (dpf). However, it was unknown whether BMP signaling was necessary for the first steps of VPB development. Thus we evaluated VPB specification by analyzing the expression of *ptf1a* and *hlxb9la* (*mnr2a*), the two first VPB markers. At 32 hpf, *ptf1a* and *hlxb9la* were absent in the pancreatic region of *alk8* mutants, whereas their expression in the neural tube remained normal (Figure 1, A, B, E, and F). However, expression of these two markers was detected a few hours later at around 38 hpf in the pancreatic region of *alk8* mutants, although in very few cells and at a reduced level compared with wild-type siblings (Figure 1, C, D, G, and H). Although *hlxb9la* was strongly reduced in the prospective VPB of *alk8* mutants at 38 hpf, its expression in the dorsal pancreatic bud was unchanged (see arrowhead in Figure 1H). In contrast to *ptf1a* and *hlxb9la*, the pan-pancreatic marker *pdx1* was not reduced in the prospective ventral bud at 30 hpf (Figure 1, I and J). Taken together, these results indicate that BMP signaling is required for the proper activation of the two ventral pancreatic genes *ptf1a* and *hlxb9la* but not for the pan-pancreatic gene *pdx1*. These data suggest that the severe pancreas hypoplasia recently reported at 72 hpf in the *alk8* mutant not only is due to an outgrowth defect of the VPB, but also results from a severe delay in its specification.

BMP signaling is required at 20 hpf to induce ventral bud specification

To determine more precisely the time window during which the BMP signaling is required to specify the VPB, we blocked this pathway using the transgenic fish *Tg(hsp70l:dnBmpr-GFP)* (Pyati *et al.*, 2005) expressing a dominant-negative form of the BMP receptor fused to

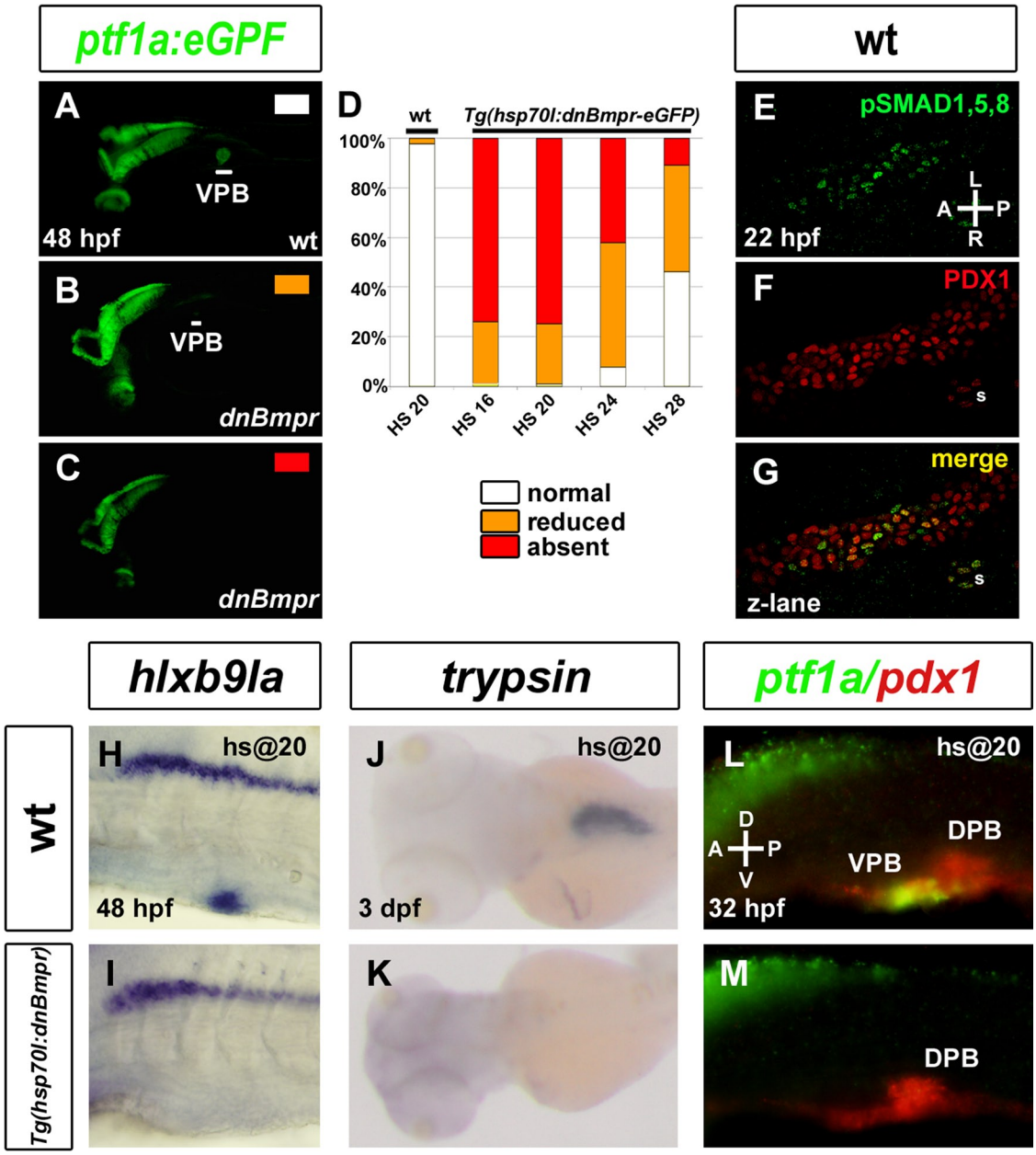

FIGURE 2: BMP signaling is essential at 20 hpf for VPB specification. (A–C, H–M) Embryos obtained from outcrossing a hemizygous *Tg(hsp70l:dnBmpr-GFP)* zebrafish with homozygous *Tg(ptf1a:eGFP)* were heat shocked at 20 hpf and harvested at 30 hpf (L, M) 48 hpf (A–C, H–I), and 3 dpf (J, K) and examined for ptf1a:eGFP fluorescence (A–C) and *hlxb9la* (H, I), *trypsin* (J, K), and *ptf1a* and *pdx1* (L, M) expression. (D) Graph quantifying ptf1a:GFP expression in wild-type and *Tg(hsp70l:dnBmpr-GFP)* heat-shocked embryos at 16, 20, 24. and 28 hpf. Data are presented as the percentage of embryos displaying normal (white), reduced (orange), or absent (red) ptf1a:GFP fluorescence. (E–G) Confocal z-lane showing activation of the BMP pathway in pancreatic cells as revealed by immunostaining with anti-pSmad 1/5/8 (green) (E) and anti-Pdx1 (red) (H) antibodies. Double pSmad 1/5/8^{+} and Pdx1^{+} cells are observed on the merge picture (G). White lines indicate the VPB. DPB, dorsal pancreatic bud; s, somite.

green fluorescent protein (GFP) under the control of the inducible heat shock promoter hsp70. These fish were crossed with *Tg(ptf1a:eGFP)* fish, and embryos from this cross were exposed to one heat shock at 16 hpf (n = 88), 20 hpf (n = 103), 24 hpf (n = 104), or 28 hpf (n = 100). Expression of the dominant-negative BMP receptor was verified after the heat shock by following the induced ubiquitous GFP expression, which was strong at 3 h and weak at 24 h after induction. Expression of ptf1a:eGFP in the ventral pancreatic region was analyzed at 48 hpf. Heat-shocked embryos could be sorted into three kinds of phenotype: unaffected (Figure 2A), strongly reduced (Figure 2B), and absent (Figure 2C) in the pancreatic region, whereas other expression domains such as eyes and brain remained unaltered. The strongest inhibition of ptf1a:eGFP in the VPB was observed in *Tg(hsp701:dnBmpr-GFP)* embryos heat shocked at 16 or 20 hpf, as 75% of transgenic embryos displayed no GFP in the VPB (Figure 2D). By contrast, heat shocking of embryos lacking the *hsp70:dnBmpr-GFP* transgene had no effect on the expression of ptf1a:GFP. Blocking BMP signaling from 24 hpf in the double-transgenic embryos still

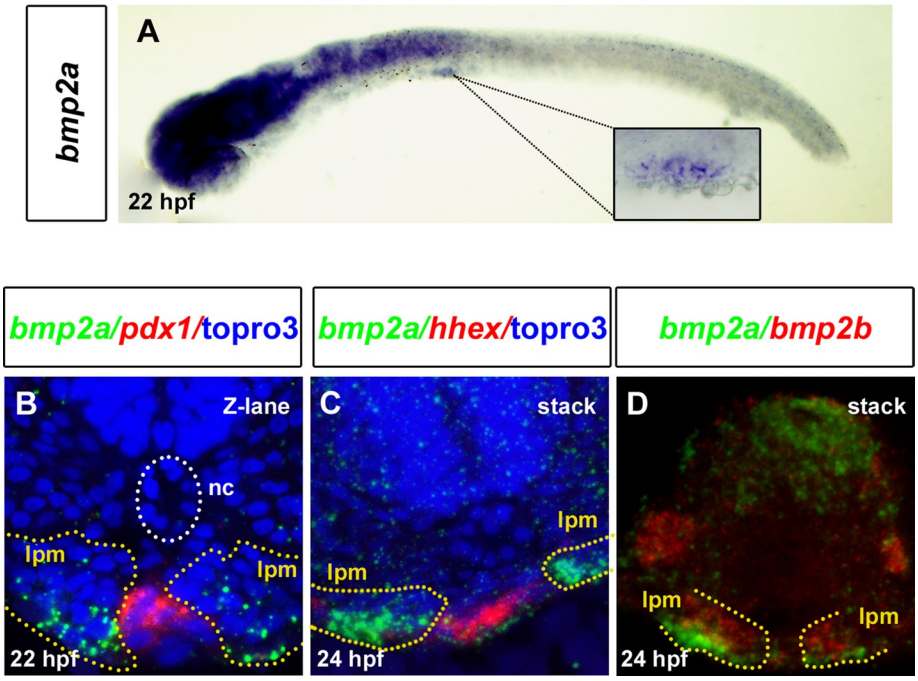

FIGURE 3: *bmp2a* is expressed in the LPM adjacent to the hepatopancreatic endoderm at 22 hpf. (A) Lateral view showing *bmp2a* expression in the LPM starting at 22 hpf. The square shows a close-up of the region indicated by the dotted lines. (B) *bmp2a* (green) and *pdx1* (red) expression analyzed by fluorescence whole-mount in situ hybridization at 22 hpf. The transverse sections were analyzed by confocal microscopy. (C) *bmp2a (green)* and *hhex* (red) expression analyzed at 24 hpf. (D) *bmp2a* (green) and *bmp2b* (red) expression comparison at 24 hpf. The images of transverse sections are flat stacking of several consecutive optical sections. TO-PRO-3 (blue) labels nuclei. Yellow and white dots delineate the LPM and the notochord (nc), respectively.

had an inhibitory effect on VPB specification, but the proportion of affected embryos was smaller compared with 16 and 20 hpf. This proportion was further reduced when the heat shock was performed at 28 hpf. These data indicate that BMP activity is required from 20 hpf onward for the specification of VPB. To determine whether, in wild-type embryos, the BMP pathway is activated in endodermal cells during this time window, we performed an immunostaining at 22 hpf with anti-phosphorylated Smad1/5/8 antibody and counterstained with anti-Pdx1 antibody to label pancreatic cells (Figure 2, E–G). Nuclear phospho-Smad 1/5/8 staining was indeed detected in some Pdx1$^+$ ventral cells, indicating that BMP pathway is activated in pancreatic cells at 22 hpf.

As for *alk8* mutants, we examined the expression of other pancreatic markers in embryos heat shocked at 20 hpf. Similar to the *ptf1a* gene, no expression of *hlxb9la* could be detected in the VPB when analyzed at 48hpf (Figure 2, H and I). Moreover, *trypsin,* a marker of the acinar pancreatic tissue—the major VPB derivative—is totally absent at 3 dpf (Figure 2, J and K). Despite the absence of *ptf1a* expression at 32 hpf after BMP inhibition, *pdx1* expression was maintained, as observed in the *alk8* mutants (Figure 2, L and M). Taken together, theses results indicate that activation of the BMP pathway in endodermal cells after 20 hpf is crucial for the induction of the early ventral pancreatic markers *ptf1a* and *hlxb9la* and for further acinar differentiation.

bmp2a is expressed in LPM adjacent to the ventral pancreatic bud and is involved in its specification

The LPM has been shown in vertebrates to be essential for proper specification of liver and pancreas (Manfroid *et al.*, 2007; Chung *et al.*, 2008). Zebrafish *bmp2a* and *bmp2b* were both reported to be expressed in LPM at 24 hpf (Chocron *et al.*, 2007; Chung *et al.*, 2008). *bmp2b* is expressed in LPM since the 10-somite stage and is required for hepatic specification at the expense of pancreatic fate, whereas *bmp2a* seems activated at later stages. Thus we investigated more closely the expression of *bmp2a* in the LPM adjacent to the prospective VPB when the BMP pathway is required for VPB specification. *bmp2a* expression starts to be detected in the LPM from 22 hpf at the level of the third somite, that is, in the hepatopancreatic region (Figure 3A), and its expression increases at 24 hpf (Figure 3C). To confirm that *bmp2a* was expressed adjacent to the pancreatic region, a double in situ hybridization with a *pdx1* probe was performed. *Bmp2a* was expressed just next to and on both sides of the *pdx1* expression domain (Figure 3B). Expression of *bmp2a* in LPM is also adjacent to the hepatic anlagen, as highlighted by *hhex* staining (shown at 24 hpf in Figure 3C). Furthermore, *bmp2a* is expressed more ventrally compared with *bmp2b* (Figure 3D) and more closely to the prospective VPB and the hepatic bud. Thus these results show that *bmp2a* is expressed at the correct time and place to be the BMP ligand responsible for proper ventral pancreatic bud specification.

To test the role of *bmp2a* in VPB specification, we performed a knockdown of its expression using a morpholino targeting the splice donor site at the *bmp2a* exon 1–intron 1 junction. The efficiency of this knockdown was checked by performing reverse transcription (RT)-PCR on RNA extracted from injected embryos using primers annealing to exons 1 and 2 of *bmp2a*. The amplified cDNA was shorter in *bmp2a* morphants compared with control embryos, and sequencing of this fragment revealed that the *bmp2a* morpholino induces a deletion of 86 base pairs in exon 1 coding sequence (Figure 4D). This deletion induces a frameshift leading to a truncated protein of 101 instead of 386 amino acids. When the ventral pancreatic markers *ptf1a* and *hlxb9la* were analyzed at 36–38 hpf in *bmp2a* morphants, absence or strong reduction of expression was noted in 69 and 73% of *bmp2a* morphants for these two genes, respectively (n = 85 and 91; Figure 4, A and B). This effect was specific to the VPB, and expression of *hlxb9la* in dorsal pancreatic bud remained unaffected (see arrowheads in Figure 4B). Expression of *insulin* and *pdx1* was not modified at 30 hpf (data not shown). As observed in *alk8* mutants, expression of *ptf1a* and *hlxb9la* was detected at later stages (48 hpf) in almost all *bmp2a* morphants but was significantly reduced compared with control embryos (data not shown). Thus these data clearly demonstrate the involvement of *bmp2a* in VPB development, with its knockdown leading to a strong delay in VPB specification.

Because several studies showed a role of BMP in induction of the hepatic bud (Shin *et al.*, 2007; Huang *et al.*, 2008) and *bmp2a* is expressed adjacent to the *hhex* expression domain (Figure 3C), we also analyzed the hepatic markers *hhex* and *prox1* in the *bmp2a* morphants. Although the expression of these two hepatic genes was still detected, their expression in the hepatic bud was clearly

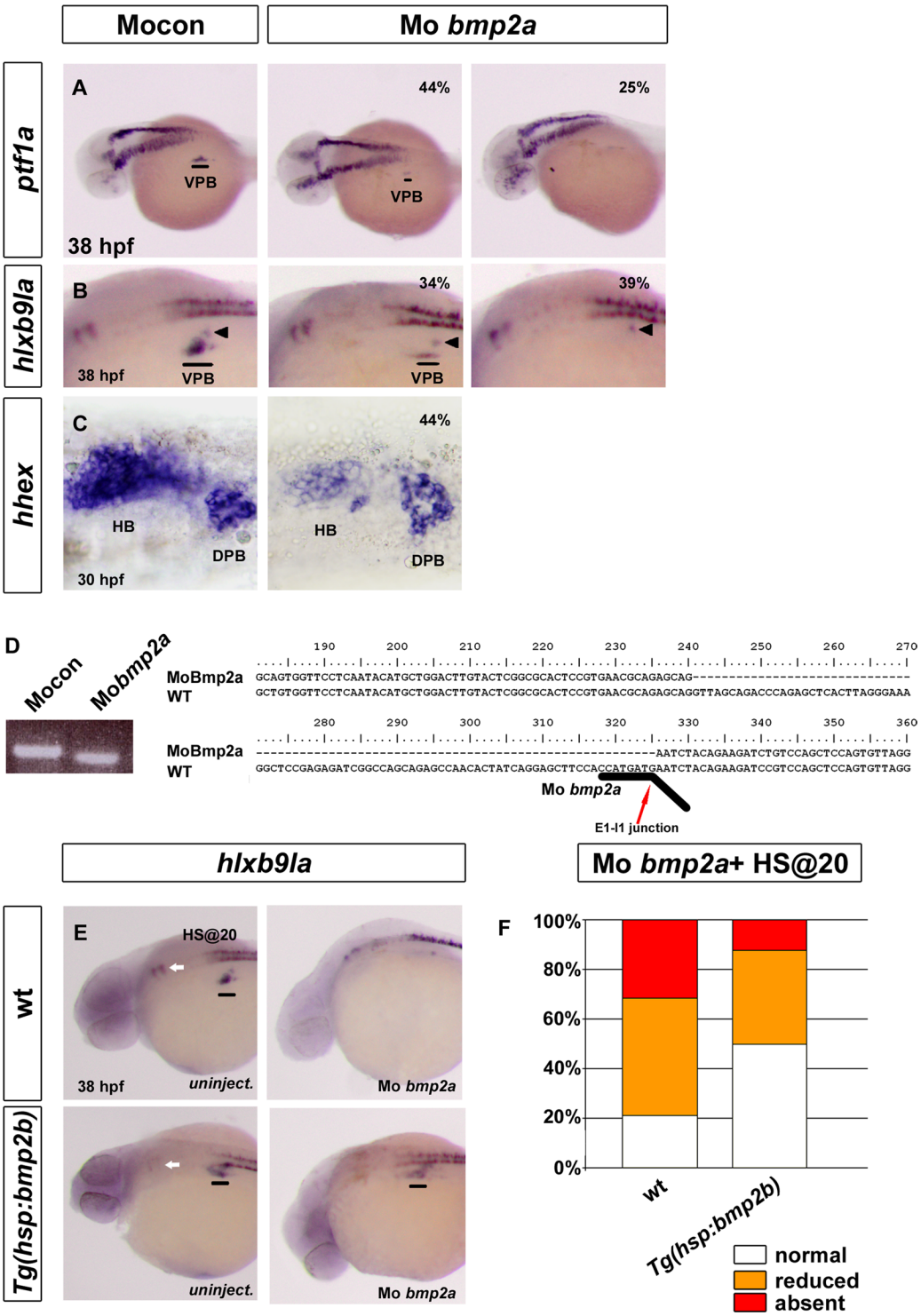

FIGURE 4: Knockdown *of bmp2a* represses VPB specification. (A–C) Analysis of ventral pancreatic and hepatic markers in control morphants (left) and in *bmp2a* morphants (right) by in situ hybridization. (A) Lateral view of *ptf1a* expression at 36–38 hpf. (B) Laterial view of *hlxb9la* expression at 36–38 hpf. (C) Ventral view of *hhex* expression at 30 hpf. Percentage represents the proportion of morphants exhibiting a reduction (middle) or an absence (right) of gene expression. (D) Gel electrophoresis after RT-PCR (left) and sequencing result (right) illustrating the RNA splicing defects caused by the *bmp2a* morpholino in injected embryos. The sequence of the amplified *bmp2a* fragment was aligned with wt *bmp2a* cDNA and revealed a 86–base pair deletion in exon 1. Black line underlines the binding site of the *bmp2a* morpholino. Red arrow shows the junction between exon 1 and intron 1. (E, F) Lateral view of *hlxb9la* expression at 38 hpf in wt and *Tg(hsp70l:bmp2b)* in uninjected embryos (E) or in *bmp2a* morphants (F). Embryos were heat shocked at 20 hpf. (G) *hlb9la* expression in wt and *Tg(hsp70l:bmp2b)* embryos injected with MO *bmp2a,* heat shocked at 20 hpf, and fixed at 38 hpf. Data are presented as the percentage of embryos displaying normal (white), reduced (orange), or absent (red) expression of *hlxb9la.* Black lines indicate the VPB; black arrowheads indicate the dorsal pancreatic bud (DPB); white arrows indicate rhombomere 5 and 6 localization. HB, hepatic bud.

reduced in 44% of morphants (n = 153) for *hhex* (Figure 4C) and in 55% of morphants for *prox1* (n = 64). These two genes were also expressed at normal level in the dorsal pancreatic bud. Thus, not only is *bmp2a* crucial for the specification of the VPB, but it is also involved in hepatic development, although it is less essential there than it is for the VPB.

To verify that the delay of the VPB specification caused by *bmp2a* morpholino is actually due to the loss of BMP2a activity, we next assessed whether induced ectopic BMP expression could rescue this defect. To activate BMP expression specifically at 20 hpf, we used the *Tg(hsp70l:bmp2b)* transgenic line allowing induction of *bmp2b* expression upon heat shock. *bmp2a* morpholinos were injected in eggs obtained from an outcross between *Tg(hsp70l:bmp2b)* and wild-type fish. Then injected embryos were heat shocked at 20 hpf, and *hlxb9la* expression was analyzed by in situ hybridization at 38 hpf. Identification of transgenic and nontransgenic embryos was performed after *hlxb9la* staining by genotyping. *Tg(hsp70l:bmp2b)* embryos also display loss of *hlxb9la* expression in rhombomeres 5 and 6 (see arrowheads in Figure 4, E and F). The rescue of *hlxb9la* expression in *bmp2a* morphants is shown in Figure 4G. The percentage of embryos exhibiting absence of *hlxb9la* expression in the pancreatic region was drastically reduced in the transgenic embryos (12%, n = 32) compared with the nontransgenic embryos (31%, n = 38). In addition, the percentage of embryos with normal *hlxb9la* expression in the VPB was significantly higher in the transgenic (50%) compared with nontransgenic (21%) embryos. Thus overexpression of *bmp2b* at 20 hpf can partially rescue the knockdown of *bmp2a*, and this indicates that the delay in VPB specification caused by the *bmp2a* morpholino is specific.

fgf10 and *24* are specifically involved in ventral pancreatic specification

Because the specification of the ventral pancreas and the development of the neighboring hepatic bud both rely on *bmp2a*, other extrinsic factors must determine the choice between the pancreatic or hepatic fate. We recently reported by morpholino knockdown experiments that *fgf10* acts redundantly with *fgf24* to control the formation of the pancreatic exocrine tissue (Manfroid *et al*., 2007). However, the role of these two FGF ligands on hepatic specification has not been investigated. Therefore we generated *fgf10; fgf24* compound mutants and examined in detail the development of the entire hepatopancreatic region. Analysis of *trypsin* and *transferrin* (*tfa*) expression at 3 dpf indicated a complete lack of the pancreatic exocrine tissue in the double mutants, whereas the liver was not reduced (Figure 5A), confirming our previous knockdown data. The absence of pancreatic exocrine tissue was due to a defect in VPB specification, as expression of *ptf1a* and *hlxb9la* was not detected in most double *fgf10; fgf24* mutants at 48 hpf (Figure 5B and data not shown). Because the VPB also gives rise to the pancreatic ducts, their formation was next analyzed in the compound mutants. Immunolabeling with Prox1, HNF4α, and 2F11 antibodies revealed complete lack of the extrapancreatic duct (EPD) connecting the pancreas to the intestine in the mutants at 50 hpf (red arrowhead). Indeed, whereas the 2F11$^+$ ductal cells delineating the extrahepatic duct (EHD) still make the junction between the hepatic bud and intestine in the mutants, extrapancreatic ductal cells could not be detected between the pancreatic islet, derived from the dorsal pancreatic bud (also 2F11$^+$), and the intestine (Figure 5D). In addition, the hepatic domain appeared posteriorly expanded toward the pancreatic endocrine islet in all mutants examined (green arrowheads; n = 6 for wild-type embryos and n = 8 for mutant embryos). Indeed, whereas the distance from the anterior limit of the hepatic bud to the islet did not significantly change (125 μm in wild-type embryos and 127 μm in mutants; yellow dotted lines), the length of the hepatic domain increased (108 μm in mutants compared with 75 μm in wild-type embryos; white dotted lines). When the double *fgf10; fgf24* mutants were analyzed at 3 dpf, no pancreatic acinar cell (Prox1$^+$) could be detected around the islet nor at intra- and extrapancreatic ducts (Figure 5, E and F). In addition, masses of ectopic hepatocyte-like (Prox1$^+$/HNF4α$^+$/2F11$^-$) cells and biliary-like cells (Prox1$^+$/HNF4α$^-$/2F11$^+$ cells) were observed contiguous to the hepatopancreatic duct remnants and also in direct contact with the gut (Figure 5, E and F). Because ectopic *tfa* expression was also noticed in this region (see white arrowhead in Figure 5A), this supports ectopic hepatic differentiation occurring posterior to the hepatic domain. Thus all these data demonstrate a complete lack of pancreatic acinar and pancreatic ductal cells in the *fgf10; fgf24* mutants, whereas hepatic cell differentiation seems increased. These results led us to examine whether, in the double mutants, specification of the hepatic bud was favored at the expense of the ventral pancreas. To that goal, we examined the expression of the hepatic marker *prox1* and of the pancreatic marker *pdx1* at 29 hpf, that is, just prior to the initiation of ventral pancreas specification (Figure 5C). Of interest, *pdx1* labeling in the ventral aspect of the pancreatic domain was dramatically reduced in all the double mutants, whereas the *prox1*$^+$ hepatic domain was expanded posteriorly and reached the dorsal pancreas (green arrowheads, n = 4). This observation suggests that, in the absence of FGF10/FGF24 signaling, hepatic progenitors are specified at the expense of the ventral pancreatic progenitors.

Because *bmp2a, fgf24*, and *fgf 10* are involved in specification of the VPB, we finally tested whether cross-regulation occurs between these extrinsic factors. Because *fgf10* expression starts in the LPM ~5 h after the onset of *bmp2a* expression (Manfroid *et al*., 2007), the activation of *bmp2a* cannot be controlled by *fgf10*. As previously reported, the *fgf24* gene displays a dynamic expression pattern, being expressed in the gut endoderm before 24 hpf, and then endodermal expression progressively decreases at the level of the pancreas, whereas it appears in the adjacent pancreatic LPM. Expression of *bmp2a* was not modified in *fgf24* mutants at 24 hpf (data not shown). Conversely, *fgf24* and *fgf10* expression was analyzed in *bmp2a* morphants. To accurately discern *fgf24* expression in the endoderm and in the LPM, double in situ hybridization was performed with *fgf24* and *pdx1* probes. Comparison of wild-type and *bmp2a* morphant embryos at 32 hpf revealed that the expression of *fgf24* is strongly decreased in the pancreatic LPM, whereas the level in the endoderm remains high (Supplemental Figure S1A). In contrast, *fgf10* expression in the LPM was not affected in *bmp2a* morphants (Supplemental Figure S1B). All these data indicate that *bmp2a* acts not only on the endoderm, but also on the mesoderm, where it is involved in the activation of *fgf24* expression.

DISCUSSION

Conflicting data have been reported on the effect of BMP and FGF signals on pancreas development, either showing a negative effect (Deutsch *et al*., 2001; Rossi *et al*., 2001; Shin *et al*., 2007; Chung *et al*., 2008; Spagnoli and Brivanlou, 2008; Tehrani and Lin, 2011) or a positive effect (Kumar *et al*., 2003; Manfroid *et al*., 2007; Wandzioch and Zaret, 2009). Studies on mouse embryonic explants first indicated that these two signaling pathways act on endodermal progenitors to favor hepatic differentiation while restricting formation of pancreatic cells (Rossi *et al*., 2001). Such role of the BMP pathway has also been confirmed in zebrafish; indeed, BMP2b secreted from the LPM around 14 hpf acts on endodermal cells to induce hepatic

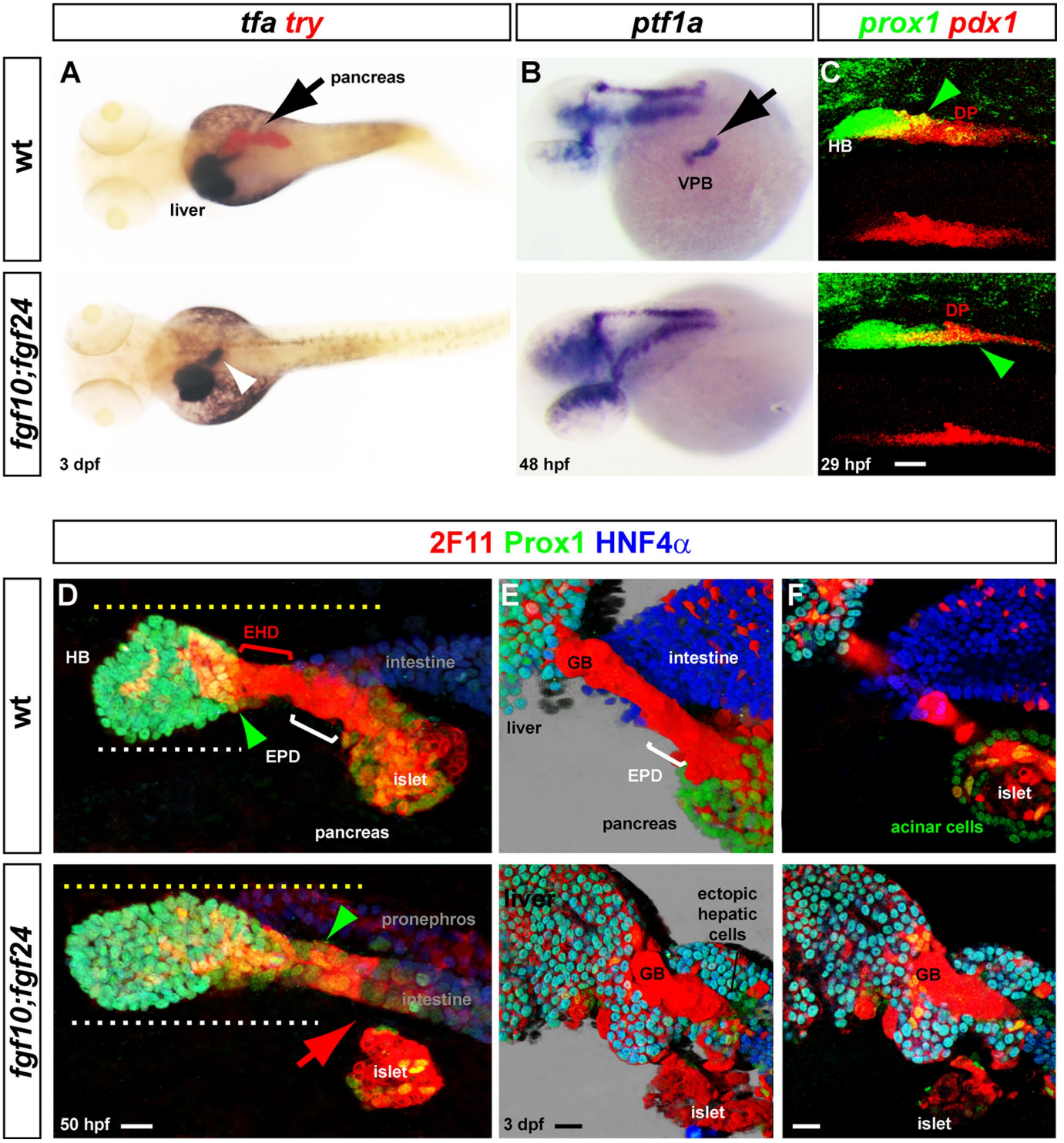

FIGURE 5: Absence of VPB cells and ectopic hepatic cells in *fgf10; fgf24* compound mutants. (A) Dorsal view of *transferrin* (*tfa*) and *trypsin* (*try*) expression, comparing wt and *fgf10; fgf24* mutants at 3 dpf. (B) Dorsolateral view of *ptf1a* expression comparing wt and double mutants at 48 hpf. (C) Confocal projection of the *pdx1* and p*rox1* expression domains at 29 hpf showing the severe decrease of *pdx1* in the anterior part of the pancreatic region and the extension of *prox1* in *fgf10; fgf24* mutants (green arrowheads). (D–F) Immunolabeling of the hepatopancreatic region with 2F11, Prox1, and HNF4α in wild-type and *fgf10; fgf24* double mutants. (D) At 50 hpf, the ventral pancreas and the EPD are absent (red arrow) in *fgf10; fgf24* mutants (confocal projections). (E, F) Morphology and differentiation of the hepatopancreatic ducts connecting the pancreas and liver to the intestine in *fgf10; fgf24* double mutants at 3 dpf. (E) Three-dimensional blend projection. (F). Z-planes). Black arrows indicate pancreas and VPB; white arrowhead indicates ectopic *tfa* expression. EHD, extrahepatic duct; EPD, extrapancreatic duct; GB, gall bladder; islet, endocrine islet. Scale bar, 20 μm.

fate at the expense of pancreas (Chung *et al.*, 2008). In the present study, we show that, a few hours later at around 20–24 hpf, the BMP pathway plays a different role and is actually essential for the specification of the ventral pancreatic bud. Furthermore, we identify BMP2a as a major BMP ligand responsible for this induction process. Similarly, FGF signaling has been shown to play a crucial role in development of liver in vertebrate (Deutsch *et al.*, 2001) and notably in zebrafish embryos between 18 and 22 hpf, that is, just before hepatic specification (Shin *et al.*, 2007). Here we demonstrate that *fgf10* and *fgf24*, also expressed in the LPM around 26 hpf and required for ventral pancreas specification, impair hepatic development. Finally, we show that *bmp2a* positively regulates *fgf24* expression in the LPM. In conclusion, our data underscore the importance of the developmental stage in the response to these extrinsic signals.

BMP signaling is crucial for ventral pancreatic specification

A recent analysis of the *alk8* zebrafish mutants revealed an increase of endocrine pancreatic β cells but also a severe hypoplasy of the ventral pancreas (Chung *et al.*, 2010). In this study, we focused our analyses on the first steps of ventral pancreatic bud development by analyzing three early pancreatic markers—*pdx1, ptf1a*, and *hlxb9la*. We show that these three pancreatic regulatory genes are differently controlled in response to BMP signaling. Indeed, whereas *pdx1* was not significantly affected in the *alk8* mutants, expression of *ptf1a* and *hlxb9la* was not detected at 32 hpf and was strongly reduced after 38 hpf in these mutants. A similar regulation was observed when BMP pathway was disrupted by two other means: first, by blocking BMP receptors after 20 hpf by using the *Tg(hsp70l:dnbmpr-GFP)* line, and second, by the knockdown of *bmp2a*.

The delay in the formation of the *ptf1a*$^+$ cells was longer after induction of the dominant-negative receptor dnBMPR-GFP than in *alk8* mutants and *bmp2a* morphants (a 16-h delay compared with 6 h). Such differences in phenotype severity are probably due to compensation by other BMP receptors I and other BMP ligands expressed at later stages. *bmp2a* expression in the LPM coincides in timing and space with the requirement of BMP for ventral pancreas specification. It is interesting to recall that its paralogue, *bmp2b*, expressed a few hours before, triggers an opposite action on pancreas specification, indeed favoring hepatic fate at the expense of pancreatic fate. This is not due to different biological activities of the two BMP2 proteins, as *bmp2a* morphant defects can be partially rescued by *bmp2b* overexpression, but rather results from a difference in their timing of expression. We can speculate that, after the genome duplication that occurred early during teleost evolution, each copy of the ancestral *bmp2* gene retained distinct regulatory sequences driving expression in the LPM either at early (for *bmp2b*) or later (for *bmp2a*) developmental stages. As in zebrafish, the critical stages of liver specification precede ventral pancreas specification, and the role of the two *bmp2* paralogues was split, with *bmp2b* acting on liver specification and *bmp2a* acting on ventral pancreas specification and on the maintenance of hepatic genes *hhex* and *prox1*.

fgf10 and *-24* specify the VPB at the expense of the hepatic fate

One important finding of our study is the role *fgf10* and *fgf24* in the induction of ventral pancreas while they restrict hepatic competence. Activation of *ptf1a* and *hlxb9la* genes in endoderm is not detected at 32 hpf in the double *fgf10; fgf24* mutants, and the *pdx1*+ domain becomes significantly reduced while the *prox1*$^+$ hepatic domain extends posteriorly. Only a delay in *ptf1a* and *hlxb9la* endodermal expression was observed either in *fgf24* homozygous mutants or in some double heterozygotes (data not shown), but expression of these two genes reappears later, around 44 hpf (data not shown). This indicates that a correct level of FGF is required for proper timing of ventral pancreas specification. At 3 dpf, the *fgf10*$^{-/-}$*; fgf24*$^{-/-}$ larvae possess only the pancreatic endocrine islet, which is derived from the dorsal bud, and no pancreatic exocrine tissue. The liver bud in these mutant larvae is apparently normal, but ectopic masses of hepatocytes develop in the endoderm just posterior to the liver, near the remnant of the hepatopancreatic ducts and close to the junction with the intestine. The actual origin of these hepatocytes is unclear; they may derive from the posterior extension of the *prox1*$^+$ hepatic domain observed at 30 hpf (Figure 3C). Two zebrafish studies recently described defects highly similar to the *fgf10; fgf24* mutant phenotype, as they showed that the endoderm posterior to the hepatic domain, corresponding to the prospective intestinal bulb and pancreas, can give rise to ectopic hepatocytes upon Wnt overexpression (Poulain and Ober, 2011; Shin *et al.*, 2011). Of interest, this hepatic competence can be induced by Wnt overexpression at 26 hpf, thus following liver specification in the hepatic progenitor domain at 22 hpf. Moreover, it is negatively regulated with time by FGF signaling (Shin *et al.*, 2011), and *fgf10a* (here referred to as *fgf10*) was shown to be partially responsible of this inhibitory effect. The present data indicate that the combined loss of *fgf10* and *fgf24*, both genes being expressed in the LPM after liver specification, is sufficient to trigger hepatic cell differentiation posterior to the normal hepatic domain without artificial Wnt overexpression. Whether Wnt signaling is activated in the *fgf10; fgf24* compound mutants remains to be elucidated.

Our data showing the ability of FGF signaling to induce pancreatic fate versus hepatic fate contrast drastically with previous data on mouse embryonic explants demonstrating the opposite effect of FGF (Deutsch *et al.*, 2001). This difference does not seem to be due to intrinsic biological activities of FGF10 and FGF24 protein ligands, as the phenotype of the *fgf10; fgf24* mutant can be almost recapitulated in wild-type zebrafish embryos treated with FGF inhibitor SU5402 between 24 and 48 hpf (data not shown; Manfroid *et al.*, 2007). In contrast, if FGF signaling is blocked at earlier stage (i.e., from 18 hpf onward), liver specification is disrupted (Shin *et al.*, 2007). This again underscores the importance of developmental stage in the response to extrinsic factors.

From data of this and other zebrafish studies, we can build a model in which hepatic versus pancreatic commitment is controlled by the sequential action of distinct extrinsic factors (Figure 6). First, *bmp2b* expressed in the LPM from 14 hpf promotes hepatic fate at the expense of pancreatic fate, notably through a down-regulation of *pdx1* in gut endoderm (Shin *et al.*, 2007; Chung *et al.*, 2008). Then, around 18–22 hpf, a FGF signal, the exact identity of which is still unknown, is required to activate *hhex* and *prox1* genes in hepatoblasts (Shin *et al.*, 2007). Activation of these two hepatic genes also necessitates Wnt2bb expression from the LPM from 22 hpf (Ober *et al.*, 2006). BMP2A is also secreted from that stage to allow activation of *ptf1a* and *hlxb9la* genes in the VPB and to maintain high expression level of *hhex* and *prox1* in hepatoblasts. Secretion of FGF10 and FGF24 from around 24–26 hpf is essential for the onset of *ptf1a* and *hlxb9la* expression determining ventral pancreatic bud. In the absence of these two FGF ligands, the *prox1/hhex*$^+$ hepatic anlagen expands posteriorly at the expense of *pdx1*$^+$ cells. Finally, our results also reveal that *bmp2a* stimulates *fgf24* expression in the pancreatic LPM. Because *fgf24* expression in the LPM, reflecting proper pancreatic LPM patterning (Manfroid *et al.*, 2007), is important for VPB specification, this thereby demonstrates that

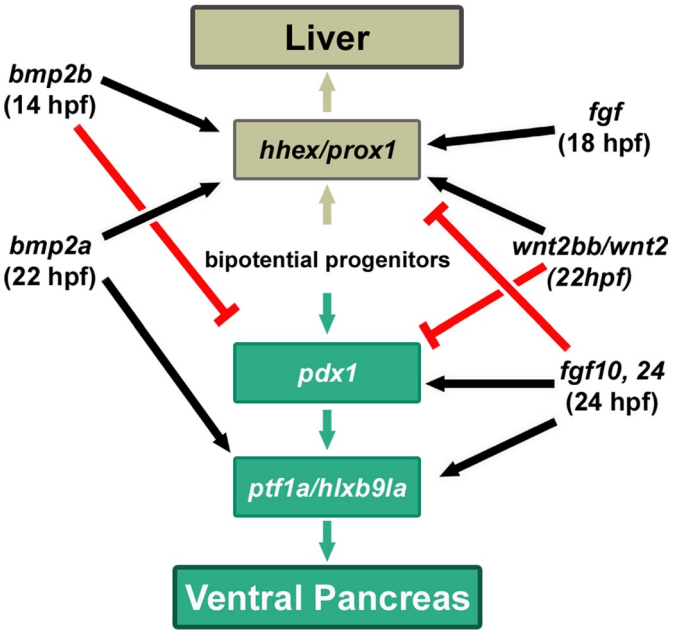

FIGURE 6: Model for the role of BMP and FGF pathways in hepatopancreatic patterning. Bipotential endodermal progenitors, shown in the center of the scheme, can give rise to liver and pancreatic cells through the consecutive action of extrinsic signals secreted from the lateral mesoderm. Hepatic specification is determined by *hhex* and *prox1* expression, whereas *pdx1*, *ptf1a* and *hlxb9la* are markers of pancreatic cell commitment.

cross-talks between BMP and FGF pathways contribute to coordinated liver and pancreas development.

MATERIALS AND METHODS

Embryos

Zebrafish (*Danio rerio*) were raised and cared for according to standard protocols (Westerfield, 1995). Wild-type embryos from the AB strain were used and staged according to Kimmel *et al.* (1995). We used the following mutant and transgenic lines: *laf*^{tm110b} (Mintzer *et al.*, 2001), *Tg(hsp70l:dnBmpr-GFP)* (Pyati *et al.*, 2005), *Tg(ptf1a:eGFP)*, (Godinho *et al.*, 2007) and *Tg(hsp70l:bmp2b)* (Chocron *et al.*, 2007).

Heat shock conditions

Embryos were heat shocked at various stages by transferring them into a prewarmed Falcon tube containing egg water in a water bath.. *Tg(hsp70l:dnBmpr-GFP)* embryos were heat shocked for 30 min at 40°C; *Tg(hsp70l:bmp2b)* embryos for 30 min at 37°C. After heat shock, embryos were transferred at 28°C and then were harvested between 30 and 72 hpf. Hemizygous *Tg(hsp70l:dnBmpr-GFP)* embryos were sorted 3 h after heat shock based on GFP-positive expression. Hemizygous *Tg(hsp70l:bmp2b)* embryos were tested for presence of the *hsp70l:bmp2b* transgene by PCR using genomic DNA after in situ hybridization, using the primers previously used Shin *et al.* (2007). In our hands, a nested PCR was needed, and the following primers were used: 5′-GCAAAAGGCCAGGAACCGTAA-3′ and 5′- GCACACAGCCCAGCTTGGAGC-3′.

Whole-mount in situ hybridization and immunochemistry

Visible in situ hybridization was performed as described (Hauptmann and Gerster, 1994). Fluorescence labeling was performed as described (Mavropoulos *et al.*, 2005).

The riboprobes used were *ptf1a* (Zecchin *et al.*, 2004), *hlxb9la* (Wendik *et al.*, 2004), *trypsin* (Biemar *et al.*, 2001), *pdx1* (Milewski *et al.*, 1998), *bmp2a* (Thisse and Thisse, 2005), *tfa* (Mudumana *et al.*, 2004), *prox1* (Glasgow and Tomarev, 1998), and *hhex* (Ho *et al.*, 1999).

Whole-mount immunohistochemistry was described in Dong *et al.* (2007). We used the following antibodies: polyclonal rabbit anti-Prox1 (1:1000; Chemicon, Temecula, CA), polyclonal rabbit anti–phospho-Smad (1:200; Cell Signaling Technology, Beverly, MA), polyclonal guinea pig against zebrafish Pdx1 (1:200; a gift from C. Wright, Vanderbilt University, Nashville, TN), polyclonal goat anti-HNF4α (1:100; Santa Cruz Biotechnology, Santa Cruz, CA), monoclonal mouse 2F11 (Crosnier *et al.*, 2005; 1:1000; a gift from J. Lewis, London Research Institute), and fluorescently conjugated Alexa antibodies (Molecular Probes, Invitrogen, Carlsbad, CA).

Fluorescence images were acquired with a Leica SP2 (Wetzlar, Germany) or Olympus FluoView FV1000 (Tokyo, Japan) confocal microscope, and three-dimensional blend projections were performed with the Imaris software (Bitplane, Zurich, Switzerland).

Injection of morpholino antisense oligonucleotides

Morpholino oligonucleotides (MOs) were purchased from Gene Tools (Philomath, OR). Each MO was resuspended in Danieau's solution at the stock concentration of 8 μg/μl. For injections, they were further diluted in Danieau's solution at 4 ng/nl with 0.5% rhodamine dextran to check injection efficiency. The splice inhibition MO *bmp2a* (AGTAAACACTTGCTTACCATCATGG) targets the exon 1–intron 1 boundary.

Control of the morpholino efficiency

Zebrafish embryos were injected at one-cell stage with Mo Bmp2a (4 ng/embryo), and mRNAs were extracted at 30 hpf. RT-PCR was performed on 1-μg mRNAs. The primers used for PCR amplification were *bmp2a* exon 1 (upstream primer; 5′-GGCTCCAGTGGACTCGTTCCTCA-3′) and *bmp2a* exon 2 (downstream primer, 5′-CTCCTGAAGAGAACCGGACGGCCT-3z), and PCR cycles were performed as follows: 40 cycles of 30 s at 94°C, 30 s at 55°C, and 30 s at 72°C, followed by a final 7-min extension at 72°C. Amplified cDNAs were analyzed by gel electrophoresis and sequencing.

Genotyping

Genotyping was performed on genomic DNA extracted from adult tails or tails obtained from embryos processed through in situ hybridization or immunohistochemistry. The *ikarus* mutation in the *fgf24* locus generates a restriction site for the *Acc*I endonuclease. The PCR fragment obtained with forward 5′-CTGTCAGTCCCACAGCAGTGGACCA-3′ and reverse 5′-CCATGTAGATTTTATTACATGTAGGT-3′ primers (615 base pairs) digested by *Acc*I produces two fragments (185 and 430 base pairs) in the mutant. The *daedalus* mutation in *fgf10* generates a single-nucleotide polymorphism that was identified by the TaqMan SNP Genotyping Assays (Applied Biosystems, Foster City, CA). The region encompassing the mutation was amplified with the forward primer dae-SNp1F 5′-CCGAGCTCCAGGACAATGTG-3′ and reverse primer dae-SNp1R 5′-GCAGGACAGACGGAACCA-3′. Allelic discrimination was performed by dae-SNp1V2 VIC primer 5′-CCCTTAGTCACTTTCCATTT-3′ (wild-type allele) and dae-SNp1M2 FAM primer 5′-CCTTAGTCACTTACCATTT-3′ (mutant allele) according to the manufacturer.

ACKNOWLEDGMENTS

We thank S. Ormenese, G. Moraes, and the GIGA-Cell Imaging Facility, W. Coppieters and the GIGA-GenoTranscriptomics Facility, and M. Winandy and the GIGA-Zebrafish Facility (Liège, Belgium).

I.M. was supported by the Fonds de la Recherche Scientifique (F.R.S.-FNRS) and by the Action de Recherches Concertées (University of Liège). B.P. and M.L.V. are Chercheurs qualifiés of the F.R.S.-FNRS. N.D. and V.V.B. are funded by Waleo (Région Wallonne). F.N. has a postdoctoral fellowship from the University of Liège. This work was funded by the Belgian State Program on Interuniversity Poles of Attraction (SSTC, PAI) and by the Sixth European Union Framework Program (BetaCellTherapy Integrated Project).

REFERENCES

Biemar F, Argenton F, Schmidtke R, Epperlein S, Peers B, Driever W (2001). Pancreas development in zebrafish: early dispersed appearance of endocrine hormone expressing cells and their convergence to form the definitive islet. Dev Biol 230, 189–203.

Chocron S, Verhoeven MC, Rentzsch F, Hammerschmidt M, Bakkers J (2007). Zebrafish Bmp4 regulates left-right asymmetry at two distinct developmental time points. Dev Biol 305, 577–588.

Chung WS, Andersson O, Row R, Kimelman D, Stainier DY (2010). Suppression of Alk8-mediated Bmp signaling cell-autonomously induces pancreatic beta-cells in zebrafish. Proc Natl Acad Sci USA 107, 1142–1147.

Chung WS, Shin CH, Stainier DY (2008). Bmp2 signaling regulates the hepatic versus pancreatic fate decision. Dev Cell 15, 738–748.

Crosnier C, Vargesson N, Gschmeissner S, Ariza-McNaughton L, Morrison A, Lewis J (2005). Delta-Notch signalling controls commitment to a secretory fate in the zebrafish intestine. Development 132, 1093–1104.

Deutsch G, Jung J, Zheng M, Lora J, Zaret KS (2001). A bipotential precursor population for pancreas and liver within the embryonic endoderm. Development 128, 871–881.

Dong PD, Munson CA, Norton W, Crosnier C, Pan X, Gong Z, Neumann CJ, Stainier DY (2007). Fgf10 regulates hepatopancreatic ductal system patterning and differentiation. Nat Genet 39, 397–402.

Field HA, Dong PD, Beis D, Stainier DY (2003a). Formation of the digestive system in zebrafish. II. Pancreas morphogenesis. Dev Biol 261, 197–208.

Field HA, Ober EA, Roeser T, Stainier DY (2003b). Formation of the digestive system in zebrafish. I. Liver morphogenesis. Dev Biol 253, 279–290.

Glasgow E, Tomarev SI (1998). Restricted expression of the homeobox gene prox 1 in developing zebrafish. Mech Dev 76, 175–178.

Godinho L, Williams PR, Claassen Y, Provost E, Leach SD, Kamermans M, Wong RO (2007). Nonapical symmetric divisions underlie horizontal cell layer formation in the developing retina in vivo. Neuron 56, 597–603.

Hauptmann G, Gerster T (1994). Two-color whole-mount in situ hybridization to vertebrate and *Drosophila* embryos. Trends Genet 10, 266.

Ho CY, Houart C, Wilson SW, Stainier DY (1999). A role for the extraembryonic yolk syncytial layer in patterning the zebrafish embryo suggested by properties of the hex gene. Curr Biol 9, 1131–1134.

Huang H *et al*. (2008). Mypt1-mediated spatial positioning of Bmp2-producing cells is essential for liver organogenesis. Development 135, 3209–3218.

Kimmel CB, Ballard WW, Kimmel SR, Ullmann B, Schilling TF (1995). Stages of embryonic development of the zebrafish. Dev Dyn 203, 253–310.

Kumar M, Jordan N, Melton D, Grapin-Botton A (2003). Signals from lateral plate mesoderm instruct endoderm toward a pancreatic fate. Dev Biol 259, 109–122.

Manfroid I, Delporte F, Baudhuin A, Motte P, Neumann CJ, Voz ML, Martial JA, Peers B (2007). Reciprocal endoderm-mesoderm interactions mediated by fgf24 and fgf10 govern pancreas development. Development 134, 4011–4021.

Mavropoulos A, Devos N, Biemar F, Zecchin E, Argenton F, Edlund H, Motte P, Martial JA, Peers B (2005). sox4b is a key player of pancreatic alpha cell differentiation in zebrafish. Dev Biol 285, 211–223.

Milewski WM, Duguay SJ, Chan SJ, Steiner DF (1998). Conservation of PDX-1 structure, function, and expression in zebrafish. Endocrinology 139, 1440–1449.

Mintzer KA, Lee MA, Runke G, Trout J, Whitman M, Mullins MC (2001). Lost-a-fin encodes a type I BMP receptor, Alk8, acting maternally and zygotically in dorsoventral pattern formation. Development 128, 859–869.

Mudumana SP, Wan H, Singh M, Korzh V, Gong Z (2004). Expression analyses of zebrafish transferrin, ifabp, and elastaseB mRNAs as differentiation markers for the three major endodermal organs: liver, intestine, and exocrine pancreas. Dev Dyn 230, 165–173.

Ober EA, Verkade H, Field HA, Stainier DY (2006). Mesodermal Wnt2b signalling positively regulates liver specification. Nature 442, 688–691.

Poulain M, Ober EA (2011). Interplay between Wnt2 and Wnt2bb controls multiple steps of early foregut-derived organ development. Development 138, 3557–3568.

Pyati UJ, Webb AE, Kimelman D (2005). Transgenic zebrafish reveal stage-specific roles for Bmp signaling in ventral and posterior mesoderm development. Development 132, 2333–2343.

Rossi JM, Dunn NR, Hogan BL, Zaret KS (2001). Distinct mesodermal signals, including BMPs from the septum transversum mesenchyme, are required in combination for hepatogenesis from the endoderm. Genes Dev 15, 1998–2009.

Shin D, Lee Y, Poss KD, Stainier DY (2011). Restriction of hepatic competence by Fgf signaling. Development 138, 1339–1348.

Shin D, Shin CH, Tucker J, Ober EA, Rentzsch F, Poss KD, Hammerschmidt M, Mullins MC, Stainier DY (2007). Bmp and Fgf signaling are essential for liver specification in zebrafish. Development 134, 2041–2050.

Spagnoli FM, Brivanlou AH (2008). The Gata5 target, TGIF2, defines the pancreatic region by modulating BMP signals within the endoderm. Development 135, 451–461.

Tehrani Z, Lin S (2011). Antagonistic interactions of hedgehog, Bmp and retinoic acid signals control zebrafish endocrine pancreas development. Development 138, 631–640.

Thisse C, Thisse B (2005). High throughput expression analysis of ZF-models consortium clones. ZFIN Direct Data Submission ZDB-PUB-051025-1.

Wandzioch E, Zaret KS (2009). Dynamic signaling network for the specification of embryonic pancreas and liver progenitors. Science 324, 1707–1710.

Wendik B, Maier E, Meyer D (2004). Zebrafish mnx genes in endocrine and exocrine pancreas formation. Dev Biol 268, 372–383.

Westerfield M (1995). The Zebrafish Book. A Guide for the Laboratory Use of Zebrafish (*Danio rerio*), 3rd ed., Eugene: University of Oregon Press.

Zecchin E, Mavropoulos A, Devos N, Filippi A, Tiso N, Meyer D, Peers B, Bortolussi M, Argenton F (2004). Evolutionary conserved role of ptf1a in the specification of exocrine pancreatic fates. Dev Biol 268, 174–184.